ACS OMEGA

Open Access

http://pubs.acs.org/journal/acsodf

Article

Ellagic Acid Induces DNA Damage and Apoptosis in Cancer Stem-like Cells and Overcomes Cisplatin Resistance

Tanima Mandal, Devendra Shukla, Subhamoy Pattanayak, Raju Barman, Rahail Ashraf, Amit Kumar Dixit, Sanjay Kumar, Deepak Kumar, and Amit Kumar Srivastava*

Cite This: *ACS Omega* 2024, 9, 48988−49000

Read Online

ACCESS | Metrics & More | Article Recommendations | Supporting Information

ABSTRACT: Cancer stem cells (CSCs) are responsible for chemoresistance and tumor relapse in many solid malignancies, including lung and ovarian cancer. Ellagic acid (EA), a natural polyphenol, exhibits anticancer effects on various human malignancies. However, its impact and mechanism of action on cancer stem-like cells (CSLCs) are only partially understood. In this study, we evaluated the therapeutic potential and underlying molecular mechanism of EA isolated from tropical mango against CSLCs. Herein, we observed that EA treatment reduces the stem-like phenotypes in cancer cells, thereby lowering the cell survival and self-renewal potential of ovarian and lung CSLCs. Additionally, EA treatment limits the populations of lung and ovarian CSLCs characterized by $CD133^{+}$ and $CD44^{+}CD117^{+}$, respectively. A mechanistic investigation showed that EA treatment induces ROS generation by altering mitochondrial dynamics, causing changes in the levels of Drp1 and Mfn2, which lead to an increased level of accumulation of DNA damage and eventually trigger apoptosis in CSLCs. Moreover, pretreatment with EA sensitizes CSLCs to cisplatin treatment by enhancing DNA damage accumulation and impairing the DNA repair ability of the CSLCs. Furthermore, EA pretreatment significantly reduces cisplatin-induced mutation frequency and improves drug retention in CSLCs, potentially suppressing the development of acquired drug resistance. Taken together, our results demonstrate an unreported finding that EA inhibits CSLCs by targeting mitochondrial function and triggering apoptosis. Thus, EA can be used either alone or in combination with other chemotherapeutic drugs for the management of cancer.

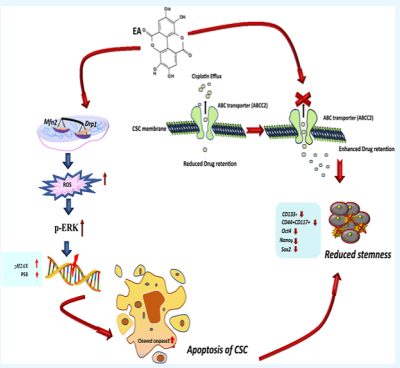

1. INTRODUCTION

Cancer is a generic term for diseases with certain hallmarks, such as rapid cell proliferation, malignancy, and neoplasm. The most common causes of cancer-related deaths are lung, colon, rectum, liver, breast, and ovarian cancer (OC).[1] Tumor relapse and chemoresistance significantly contribute to many cancer-related deaths.[2] Several studies demonstrated that cancer stem cells (CSCs) contribute to development of secondary tumor and chemoresistance.[3] Conventional chemotherapeutics fail to eliminate the CSC pools. There is an urgent requirement to develop a therapeutic strategy to eradicate the CSC population.

Phytochemicals are plant-derived, natural, biologically active chemicals synthesized by plants as a natural defense against pathogens and predators[4] and widely used in treating various diseases, including cancer.[5] Ellagic acid (EA) is a dietary polyphenol that belongs to the ellagitannin family (ETs). It may be present in either free form or as ellagitannin in a variety of edible plants such as mango, strawberries, cranberries, blueberries, edible mushrooms, pomegranate, grapes, walnuts, tea, *etc.*[6−8] After consuming EA-containing plants/plant products, human gut microbiota metabolizes the ETs and EA into urolithins.[9] Previous studies have demonstrated the anti-inflammatory and anticancer activities of EA and urolithins.[10,11] Additionally, it is widely believed that combination therapy could improve cancer treatment by addressing the concern of chemoresistance and reduced drug sensitivity.[12] Additionally, combinatorial drug therapy lessens the toxicity induced by traditional anticancer chemotherapeutics drugs. Several studies have demonstrated that cisplatin is used in conjunction with other medications to overcome its toxicity.[13] Combinatorial drug therapy is a better alternative to combating the disease crisis.

Nonsmall cell lung carcinoma (NSCLC), and ovarian cancer account for the most deaths because of low sensitivity to conventional chemotherapy.[14] Tumor relapse is one of the primary reasons for low survival rate in the past few years.[15] *Mangifera indica* contains a higher amount of EA.[16] Thus, we used *M. indica* seeds to isolate EA and characterize it. Furthermore, we studied the therapeutic potential and

Received: November 6, 2023
Revised: December 28, 2023
Accepted: January 3, 2024
Published: December 5, 2024

underlying molecular mechanism of EA against ovarian and lung CSLCs using *in vitro* 2D and 3D models.

2. METHODS AND MATERIALS

2.1. Isolation and Characterization of EA. The seeds of the plant were collected from the locality of Jadavpur-Kolkata in July 2018 and authenticated as *M. indica* L. by the Central National Herbarium, Botanical Survey of India, Howrah. A herbarium specimen is preserved in the laboratory for future reference (IICB/DK/001). The fresh seeds were cut into pieces (300 g) and extracted with methanol at room temperature (1000 mL × 3; 72 h each time). The resultant extract was filtered and concentrated to afford the methanolic extract (90 g), which was further fractionated into ethyl acetate and aqueous fractions. The ethyl acetate fraction (30 g) was chromatographed over diaion HP20 and eluted with water: methanol (50:50; 3 L; 100 mL fractions) and methanol (2.25 L; 50 mL fractions). Based on TLC analysis, fractions 3−8, 9−14, 15−32, 33−34, 35−40, and 41−58 were mixed. Mixed fraction 9−14 (9.2 g) led to the isolation of a pale yellow-colored amorphous solid (2.2 g), which displayed a single spot-on TLC. The isolated compound was subjected to spectroscopic characterization:

[ESI-MS +ve: 303.0128 $[M + H]^+$; ^1H NMR (DMSO-d_6, 400 MHz): 7.46 (1H, s); ^{13}C NMR (DMSO-d_6, 100 MHz): δ 159.16 (−C), 148.14 (−C), 139.60 (−C), 136.41 (−C), 112.34 (−C), 110.26 (−CH), 107.68 (−C)] (Figures S1−S3).

2.2. HPLC Analysis. The isolated EA was subjected to purity analysis using Ascentis C18, 25 cm × 4.6 mm, 5 μm column as the stationary phase and a gradient of A: water (0.1% formic acid) and B: acetonitrile {A/B—90:10 v/v (0 min); 50:50 v/v (20 min); 50:50 v/v (23 min); 90:10 v/v (25 min); 90:10 v/v (30 min)} as the mobile phase (1 mL/min) using a Shimadzu HPLC system (Figure S4).

2.3. Cells and Reagents. A549 (lung cancer), A2780, and SKOV3 cells (ovarian cancer) were generously provided by Prof. Ramesh Ganju's lab, The Ohio State University, Columbus, USA. The C13 cell line was provided by Prof. Qi-En Wang, The Ohio State University, Columbus, USA. These cells were cultured in the recommended RPMI medium (Gibco) and supplemented with 0.5% penicillin/streptomycin (Gibco) and 10% fetal bovine serum (Gibco). The cells were maintained in a 5% CO_2 incubator at 37 °C. Additionally, A549 cells were sorted using anti-CD133 beads through the MACS column (Miltenyi Biotec). A mycoplasma test was conducted using a kit (Lonza) at regular intervals before performing experiments. Cell lines below passage number 20 were used for the study. Cisplatin was purchased from Sigma-Aldrich.

2.4. Spheroid Formation Assay. SKOV3 and A549 cells were cultured in a 6-well ultralow dish (Corning) at a density of 1000 cells per well with CSC-specific media containing DMEM/F12 Knockout media, 20% knockout serum replacement (Gibco) and growth factors such as 10 ng/mL bFGF, 10 ng/mL EGF, and insulin. The cells were maintained at 37 °C in a 5% CO_2 incubator. After 7 days, spheroids were treated with various concentrations (0, 5, 10, 25, and 50 μM) of EA dissolved in DMSO for 48 h, while DMSO (0.5% v/v) treatment was used as a vehicle control. Darkfield images of spheroids were captured by the Olympus CKX53 inverted microscope.

2.5. Cell Viability Assay. Adherent A549 and SKOV3 cells, as well as CSLCs, were seeded at a density of 5000 cells/well in regular and ultralow attachment 96-well plates, respectively. A549 and SKOV3 cells were treated with various doses of EA dissolved in DMSO, such as 5, 10, 25, and 50 μM for 24 h. CSLCs were treated with EA (5, 10, 20, and 50 μM) for 24 h. DMSO (0.5%, v/v) was used as a vehicle control. The media were removed, and the cells were washed with PBS. MTT solution at a final concentration of 5 mg/mL was added per well and incubated for 4 h. Afterward, 100 μL of DMSO was added to each well of a 96-well plate and kept on a shaker for 10 min. O.D. (570 nm) was measured using a MultiSkan FC microplate photometer (Thermo Fisher Scientific, Inc.).

2.6. Live−Dead Assay. A549-CD133$^+$ and SKOV3-spheroids were cultured in an ultralow attachment six-well plate (Corning) at a density of 0.2 × 10^6 cells/well. CSLCs were treated with various doses of EA (5, 10, 25, and 50 μM) for 48 h. Additionally, CSLCs were pretreated with a lower concentration of EA (5 μM) for 24 h, followed by cisplatin (10 μM) for 12 h for combinatorial studies. Furthermore, the cells were incubated in fresh medium for an additional 36 h. Afterward, the medium was removed and cells were washed with 1× chilled PBS. Cells were stained with propidium iodide (5 μM) and acquired by BD FACS Diva located at the CSIR-IICB TRUE campus. Data were reanalyzed by FlowJo software.

2.7. Flow Cytometry Analysis of Stem Cell Markers. Anti-CD117 PE-conjugated (Miltenyi Biotec cat. no. 130-127-173), anti-CD44 FITC-conjugated (Miltenyi Biotec cat. no. 130-113-903) for SKOV3, and anti-CD133 PE-conjugated (Miltenyi Biotec cat. no. 130-110-962) for A549 were used for flow cytometric analysis to determine the percentage of CSCs present within the cancer cells. Following treatment with EA, cisplatin, or a combination, cells were stained with antibodies and incubated in the dark for 30 min at 4 °C. Subsequently, cells were washed with PBS and resuspended in 250 μL of 2% BSA and analyzed using flow cytometry BD FACS Diva. Data were reanalyzed by FlowJo software.

2.8. Real-Time PCR Analysis. CSLCs were treated with either DMSO or EA (25 μM) for 48 h. TRIzol reagent (Invitrogen cat. no. 15596026) was used to isolate the total RNA. Further, cDNA synthesis was carried out using a cDNA reverse transcription kit (Applied Biosystems cat. no. 4368814) and followed by qPCR using Fast SYBR Green PCR Master Mix (Applied Biosystems cat. no. 4385612) on the QuantStudio 3 Real-Time PCR System applied biosystem located at the central facility of the CSIR-IICB TRUE campus with the following primers: Sox2, forward, 5′-ACCGTGATGCCGACTAGAAA-3′, reverse, 5′-GCGCCTAACGTACCACTAGAA-3′; Oct4, forward,5′-GAAGTTGGAGAAGGTGGAACC-3′, reverse, 5′-CCTTCTGCAGGGCTTTCATA-3′; Nanog, forward, 5′-TGCTACTGAGATGCTCTGCAC-3′, reverse5′-GGGCTATCTTGAAGAGGTAGGTC-3′; ABCC2, forward,5′-AGTGAATGACATCTTCACGTTTG-3′, reverse, 5′-CTTGCAAAGGAGATCAGCAA-3′ 18S, forward, 5'-GCAATTATTCCCCATGAACG-3' , reverse, 5'-TGTACAAAGGGCAGGGACTTA-3'.

2.9. Determination of the Intracellular ROS Level. A549-CD133$^+$ and SKOV3- spheroids (0.5 × 10^6) cells were seeded in a 6-well ultralow attachment dish (Corning) with a cancer stem cell-specific medium. Cells were treated with either DMSO or EA (5, 10, and 25 μM) for 24 h. Intracellular ROS levels were measured using a commercially available kit (ENZO cat. no. 51011) as per the protocol suggested by the

https://doi.org/10.1021/acsomega.3c08819
ACS Omega 2024, 9, 48988−49000

manufacturer. Briefly, cells were stained with the ROS detection reagent (2,7-dichlorofluorescein diacetate dye) and acquired by flow cytometry.

2.10. γH2AX Detection. To quantify the extent of DNA damage, A549-CD133$^+$ and SKOV3- spheroids were treated with various doses of EA for 48 h, while control cells were treated with DMSO alone. The single-cell suspension obtained from spheroids *via* gentle pipetting was fixed in 4% paraformaldehyde. Further, cells were permeabilized with the help of 0.1% Triton-X and incubated on ice for 10 min. Washing was done twice with 1× PBS and staining was performed using the γH2AX (Miltenyi Biotec cat. no. 130-130-829) antibody. Cells were resuspended into 250 μL of PBS and analyzed through flow cytometry.

Furthermore, a DNA repair kinetics study was performed following the treatment of CSLCs with DMSO, EA, cisplatin, and combination. After 12 h of treatment, cells were allowed to recover for 3 h and were then fixed, permeabilized, washed, and stained as per the protocol mentioned above. The percentage of γH2AX formation was determined by using flow cytometry.

For immunofluorescence studies, cells were grown on coverslips in a 6-well plate at a density of 2 × 10^5 cells/well and allowed to adhere for 24 h. Cells were treated with EA, cisplatin, or a combination of both. Coverslips were removed with the help of sterile forceps and washed with 1× PBS, and cells were fixed with 4% paraformaldehyde. Cells grown on coverslips were stained with the γH2AX antibody (Cell Signaling Technology cat. no. 9718S) and images were acquired with a confocal microscope (Zeiss, LSM 980) located at the central facility of CSIR-IICB, TRUE campus, Kolkata.

2.11. Live−Dead Imaging. The cells were seeded in a 6-well ultralow attachment plate at the density of 10,000 cells per well and grown in CSC media for 10 days. Spheroids were treated with various concentrations of EA for 48 h. After that, the cells were washed with 1× PBS and then resuspended in CSC media lacking serum. CFDA dye (Invitrogen cat. no. V12883) and PI stain were added to the cells and kept for incubation for 20 min in the dark. The images were acquired by a ZOE fluorescence imager (Bio-Rad, USA).

2.12. Colony Formation Assay. A549 and SKOV3 cells were grown at a density of 0.2 × 10^6 cells/60 mm dish in 3 mL of RPMI complete media. After 24 h, EA solution (5, 10, 25 μM) was added to the cells and incubated for 24 h after which cells were seeded at a density of 1000 cells/well in the 6-well plate with a fresh complete culture medium. After 10 days, A549 and SKOV3 cells were fixed for 45 min in 4% paraformaldehyde solution (Sigma-Aldrich) and stained with 0.5% (v/v) methylene blue (Sigma-Aldrich USA) for 3 h. Colonies obtained were counted and the results were expressed in terms of colony formation efficiency (CFE) % = {(no. of colonies counted/no. of cells seeded) × 100}.

2.13. Immunoblotting. SKOV3, A2780, and A549 spheroids were treated with EA for 48 h. After that, whole cell lysate was extracted by sonicating the CSLCs aggregate in a RIPA buffer. The obtained protein samples were quantified, and equal amounts of proteins were resolved by using SDS-PAGE and then transferred to a methanol-activated PVDF membrane. Protein bands were immunodetected using anti-p53 (Cell Signaling Technology: CST cat. no. 2527T), anti-Cleaved Caspase3 (CST cat no. 9664T), anti-pERK (Santa Cruz 7383), antitotal-ERK (CST cat no. 9102S), anti-Mfn2 (CST cat. no. D2D10), anti-Drp1 (CST cat. no. 8570), anti-GAPDH (CST cat. no. 2118S), and anti-β-actin (CST cat. no. 4970).

2.14. Annexin V/PI Assay. A549-CD133$^+$ cells were seeded at a density of 0.2 × 10^6 per well in a 6-well ultralow attachment plate and grown in CSC selective media for 10 days. The spheroids formed were treated with various doses (0, 5, 10, 25 μM) of EA for 48 h. The cells were pipetted gently to get single cell suspension and centrifuged for 5 min at 1500 rpm, then resuspended into binding buffer, and then Annexin V and PI (BD Biosciences cat. no. 556547) stains were added and incubated in the dark for 15 min and subjected to flow cytometry analysis.

2.15. Hypoxanthine-Guanine Phosphoribosyl Transferase Mutagenesis Assay. The hypoxanthine-guanine phosphoribosyl transferase (HPRT) mutagenesis assay was performed following the method described by Zhu et al.,.[17] Briefly, A549 cells were treated with EA (5 μM), cisplatin (10 μM), or pretreated with EA (5 μM) followed by cisplatin (10 μM). The cells were then selected for HPRT mutants by treating them with 6-thioguanine (6-TG) for 10 days. Afterward, the cells were fixed in 4% paraformaldehyde and stained with 0.5% methylene blue. The number of 6-TG-resistant clones was then counted.

2.16. Statistical Analysis. One-way ANOVA and unpaired Student's *t*-test were performed to analyze the data. The data were represented as mean ± SD with a significance level of $p < 0.05$.

3. RESULTS

3.1. Isolation and Characterization of EA. The ethyl acetate fraction after purification resulted in the isolation of one major compound. The isolated compound was characterized as EA by comparing the NMR data with those reported in the literature.[18] Additionally, on HPLC analysis, it was found to be more than 99% pure (Figure S4).

3.2. Isolation and Characterization of the Lung and Ovarian CSLCs and Anticancer Activity of EA. Cancer cells, when grown in a serum-free medium added with specific growth factors form spheroids, exhibiting enriched CSCs properties.[19] Similar to previous report,[20] A549-CD133$^+$ cells were sorted from the A549 cell line with the help of magnetic beads (Miltenyi Biotec cat. no. 130-100-857) as per protocol provided by the manufacturer. Numerous studies have demonstrated that CD133$^+$ could be considered as cancer stem-like cells in lung cancer.[20] SKOV3 cells were grown in CSC-specific media to develop SKOV3- spheroids, exhibiting enhanced stem cell-like properties (Figure S5A−C). Higher expression of stem cell markers such as Nanog, Oct-4, and Sox-2 and lower levels of reactive oxygen species (ROS) were noticed in CSLCs (A549-CD133$^+$ and SKOV3- spheriods) compared to their bulk cells (A549 and SKOV3) (Figure S5D−I). The cytotoxic activity of pure EA was assessed on spheroids enriched with CSC-like (3D) cells and bulk (monolayer) cells in SKOV3 and A549 after 24 h of treatment, respectively. The MTT assay also confirms the higher resistant phenotype of A549-CD133$^+$ (IC_{50} 53.63 μM) and SKOV3-spheroids (IC_{50} 47.43 μM) compared to A549-CD133$^-$(IC_{50} 17.44 μM) and SKOV3 (IC_{50} 19.4 μM) adherent cells, respectively (Figure S6A,B). The clonogenic assay showed a reduced colony-forming efficiency in cells subjected to EA treatment, further confirming the cytotoxicity of EA against cancer cells (Figure S7A,B).

https://doi.org/10.1021/acsomega.3c08819
ACS Omega 2024, 9, 48988−49000

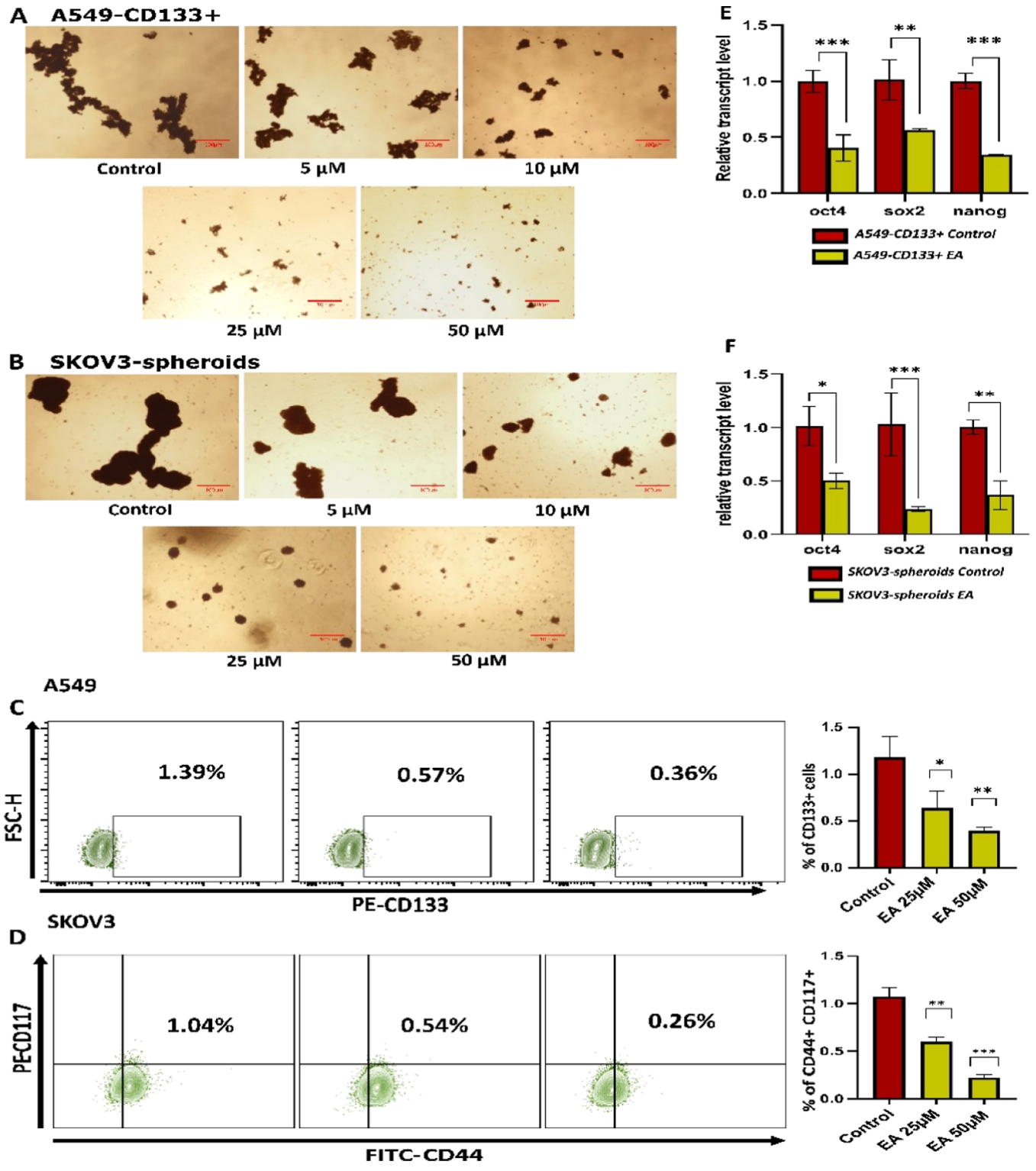

Figure 1. EA treatment reduces lung and ovarian CSLCs *in vitro*. Representative images of A549 $CD133^+$ (A) and SKOV3- spheroids (B) treated with different doses of EA (0−50 μM) for 48 h. Scale bar = 100 μm. (C) A549 and (D) SKOV3 cells were treated with either DMSO or EA (25 and 50 μM) for 24 h, further cells were incubated in fresh medium for an additional 24 h. Flow cytometry analysis was performed to analyze the percentage of $CD133^+$ and $CD44^+CD117^+$, respectively. Representative contour plots showing $CD133^+$ and $CD44^+CD117^+$ populations in corresponding graphs, respectively. (E,F) EA treatment (25 μM for 48 h) significantly reduces the expression of stem cell markers genes such as Oct4, Sox2, and Nanog in CSLCs. N=3, Bar, SD; *$P < 0.05$, **$P < 0.01$ and *** ($P < 0.001$).

3.3. EA Treatment Depletes Lung and Ovarian CSLCs *In Vitro*.

It has been reported that $CD133^{+}$[20] and $CD44^+CD117^{+}$[21] are believed to be typical surface stem cell markers for A549 and SKOV3 cells, respectively. Furthermore, CSC-enriched cell populations display enhanced sphere formation ability and resistance to chemotherapeutic agents. To assess the impact of EA on CSLC cells, A549 $CD133^+$ and SKOV3 spheroids treated with EA (0, 5, 10, 25, or 50 μM) for

https://doi.org/10.1021/acsomega.3c08819
ACS Omega 2024, 9, 48988−49000

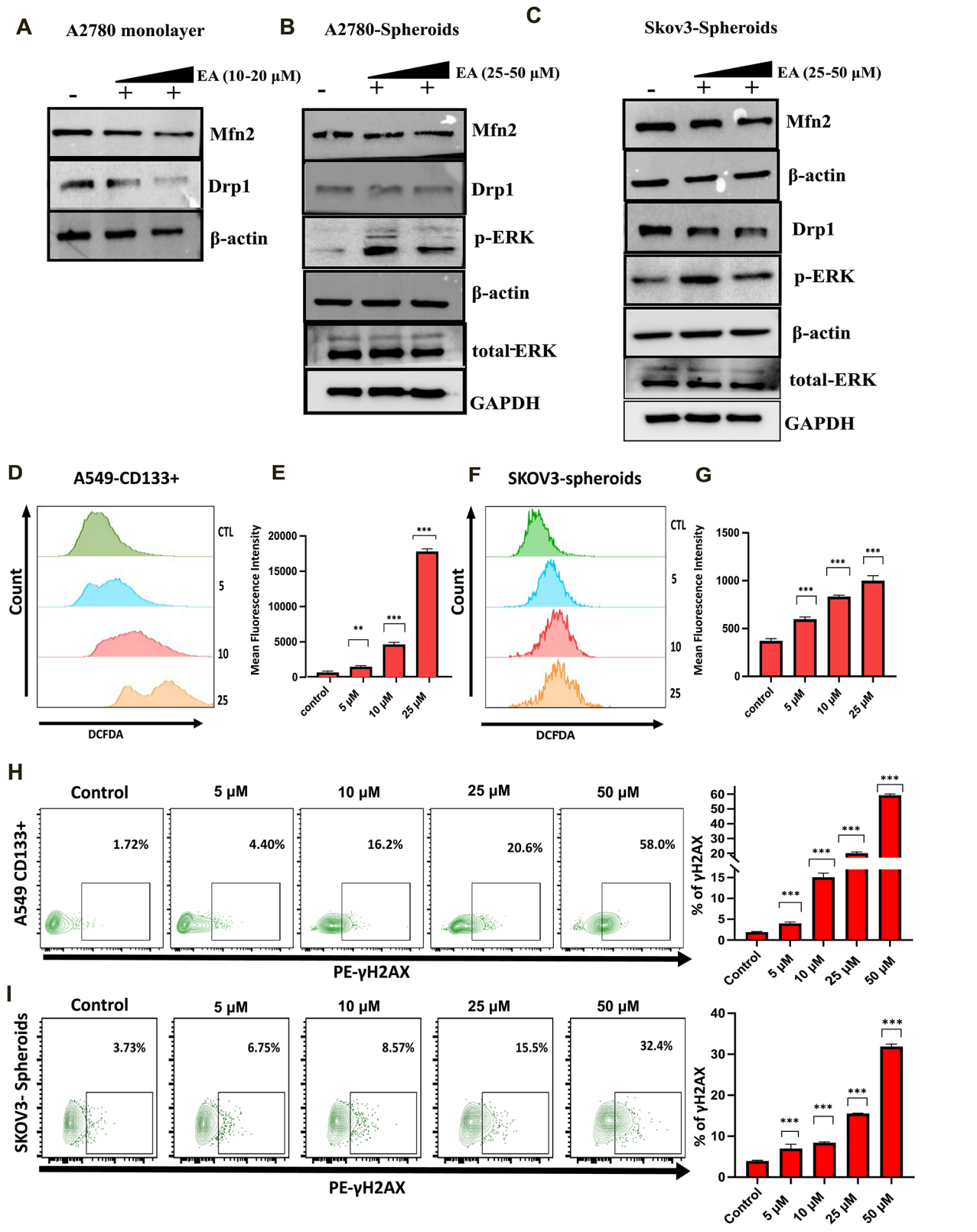

Figure 2. EA treatment alters mitochondrial dynamics, leading to the accumulation of intracellular ROS and DNA damage. Western blot analysis of the protein levels of Mfn2, Drp1, total-ERK, and p-ERK in the (A) A2780 monolayer, (B) A2780 spheroids, and (C) SKOV3 spheroids cells; A549-CD133$^+$ (D,E) and SKOV3- spheroids (F,G) were treated with different concentrations of EA (0, 5, 10, 25 μM) for 24 h. Intracellular ROS accumulation was determined using flow cytometry. Representative histograms and corresponding bar diagrams showing ROS level in CSLCs; A549-CD133$^+$ (H) and SKOV3- spheroid (I) cells were treated with different doses of EA for 48 h. γH2AX accumulation was detected through flow cytometry to evaluate the extent of DNA damage induced by EA. Representative contour plots obtained from flow cytometry analysis showing the percentage of γH2AX positive cells. Data was reanalyzed using FlowJo software. In all graphs, the results are represented as mean ± SD of triplicate experiments. $^{**}P < 0.01$, and $^{***}P < 0.001$.

https://doi.org/10.1021/acsomega.3c08819
ACS Omega 2024, 9, 48988−49000

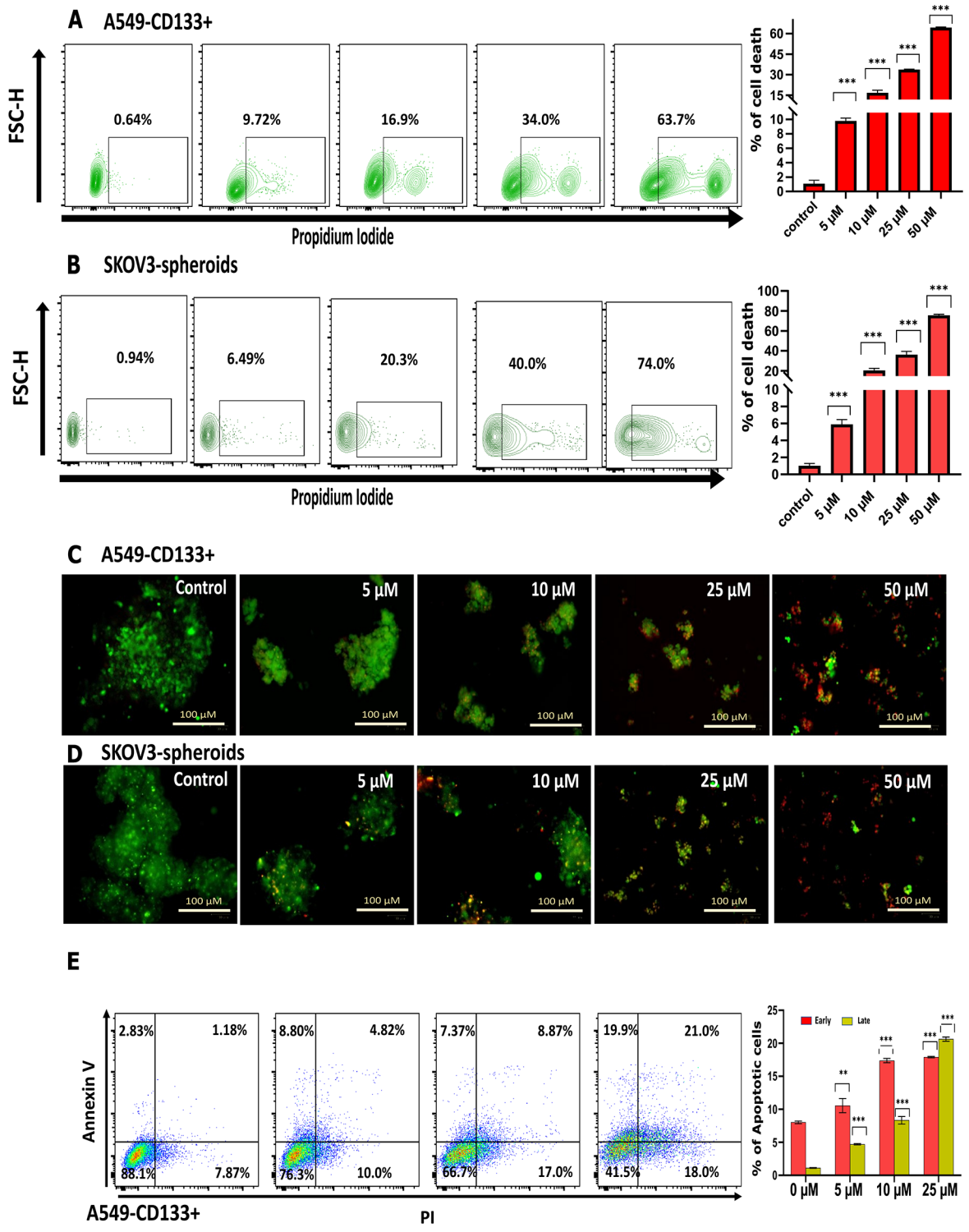

Figure 3. EA treatment induces cell death in lung and ovarian CSLCs *via* inducing apoptosis A549-CD133$^+$ (A) and SKOV3 spheroids (B) were treated with different doses (0−50 μM) of EA for 48 h. The percentage of cell death was determined using flow cytometry. Representative contour plots obtained from flow cytometry analysis showing the percentage of dead cells. Data were reanalyzed using FlowJo software. Live−dead staining using CFDA (green) and propidium iodide (red) following EA treatment (0, 5, 10, 25, 50 μM) in A549-CD133$^+$ cells (C) and SKOV3- spheroids (D). Images were captured with a ZOE fluorescence microscope (Scale bar = 100 μm). Reanalysis was performed using ImageJ software. The A549-CD133$^+$ (E) were treated with different doses of EA (0, 5, 10, 25 μM) for 48 h. Viable cells, early apoptotic, and late apoptotic cells were represented by the lower left quadrant (Annexin-V$^-$/PI$^-$), lower right quadrant (Annexin-V$^+$/PI$^-$), and upper right (Annexin-V$^+$/PI$^+$) quadrant, respectively. The corresponding graph shows the percentage of early and late apoptotic cells following EA treatment. N=3, Bar, SD;$^{**}P < 0.01$, and $^{***}P < 0.001$.

48 h were imaged using a microscope (Olympus microsystem imager). As depicted in Figure 1A,B, less remarkable changes in the dimensions and morphology of the spheroids were observed at lower concentrations (5 μM), whereas increasing

https://doi.org/10.1021/acsomega.3c08819
ACS Omega 2024, 9, 48988−49000

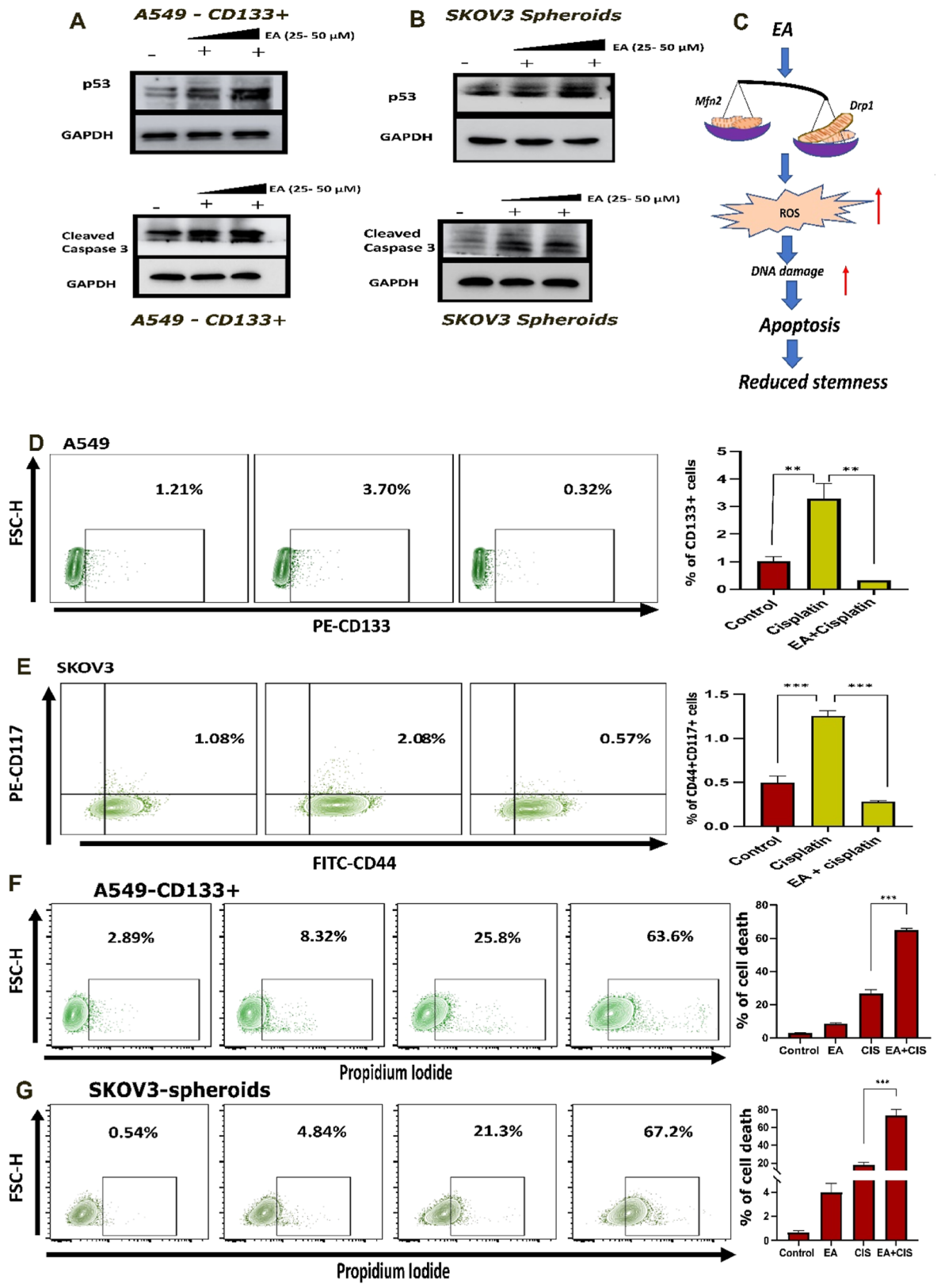

Figure 4. EA triggers the pro-apoptotic pathway in CSLCs. The combinatorial treatment of EA and cisplatin blocks cisplatin induced-CSLCs enrichment and enhances cell death in CSLCs. Western blot analysis of the protein levels of p53 and cleaved caspase 3 in A549-CD133$^+$ (A) and SKOV3- spheroids (B) following EA treatment. (C) The schematic diagram highlights the possible pathway for EA-induced apoptosis and CSC depletion. Pretreatment of EA (5 μM for 24 h) followed by cisplatin treatment (10 μM for 12 h) significantly blocked the enrichment of CSLCs. Representative contour plots showing (D) CD133$^+$ and (E) CD44$^+$CD117$^+$ percent enrichment through flow cytometry analysis. DMSO, EA, cisplatin, and EA + cisplatin treatment-induced cell death in (F) A549-CD133$^+$ and (G) SKOV3 spheroid cells was analyzed through flow cytometry. N=3, Bar, SD; $^{**}P < 0.01$, and $^{***}P < 0.001$.

https://doi.org/10.1021/acsomega.3c08819
ACS Omega 2024, 9, 48988−49000

concentrations of EA (10, 25, and 50 μM) led to a significant change in the size and morphology of the spheroids compared to the vehicle control. This indicates the inhibitory effects of EA on the sphere formation ability, which is a key property of CSCs. To further validate the effect of EA on the lung and ovarian CSC properties, we determined the percentage of A549-CD133$^+$ and SKOV3-CD44$^+$CD117$^+$ cells after treatment with EA (25 and 50 μM) for 24 h, respectively. Our data showed that EA treatment reduces the abundance of CSLCs in a dose-dependent manner *in vitro* (Figure 1C,D), indicating that EA can disrupt lung and ovarian CSCs.

CSCs exhibit elevated expression of stem cell marker genes, such as Nanog, Sox2, and Oct4, important for self-renewal, proliferation, and maintenance of the embryonic stem cell population.[22] To determine if EA can inhibit the expression of these stem cell markers in CSLCs, we sorted A549-CD133$^+$ and A549-CD133$^-$ cells from the A549 cell line using magnetic beads. Additionally, SKOV3 spheroids were developed by growing SKOV3 cells in cancer stem cell-specific medium for 10 days. Subsequently, these cells were then treated with either DMSO or EA for 48 h. As shown in Figure 1E,F, EA treatment considerably reduced the expression of stem cell marker genes.

3.4. EA Treatment Alters Mitochondrial Dynamics and Induces ROS Generation in Ovarian and Lung CSLCs. To assess whether EA treatment induces changes in mitochondrial dynamic regulators, we treated A2780 monolayer cells, A2780 spheroids, and SKOV3 spheroids with varying concentrations of EA. Western blot analysis confirmed that EA induces significant alterations in Drp1 expression in a concentration-dependent manner (Figure 2A−C). Additionally, slight changes in Mfn2 expression were also observed.

Mitochondrial dynamics, a balanced fission and fusion event, determine mitochondrial morphology, which, in turn, shapes mitochondrial functions. The fission process is regulated by Drp1, recruited by adapter proteins such as Fis1, Mid-49, and 51, while Mfn1 & 2 and OPA1 control fusion events. Any disturbance in the balance of these events can lead to mitochondrial dysfunction. Notably, mitochondrial fusion and fission proteins likely impact cancer dynamics, at least partially through the regulation of ROS activity. The expression of mitochondrial fission and fusion proteins correlates with ROS generation.[23]

An excessive intracellular ROS buildup causes damage to DNA, proteins, lipids, membranes, and organelles, leading to apoptosis of cells. To determine whether EA treatment induces ROS generation in lung and ovarian CSLCs, A549-CD133$^+$ and SKOV3- spheroid cells were treated with EA and subjected to FACS analysis. As shown in Figure 2D,F, EA treatment resulted in a concentration-dependent, substantial increase in ROS generation in both cancer types. In fact, compared to the control, the intracellular ROS accumulation for the 25 μM treatment dose was around -20 and 2.25-folds higher in A549-CD133$^+$ and SKOV3- spheroids, respectively.

3.5. EA Treatment Induces DNA Damage Accumulation in Lung and Ovarian CSLCs. The phosphorylation of histone variant H2AX at the serine-139 position (γH2AX) induces the formation of nuclear foci at the site of damage and is considered a well-known marker of DNA damage. It is known that the phosphorylation of the histone variant H2AX is a prerequisite for apoptotic DNA fragment formation.[24] γH2AX formation after EA treatment was examined in CSLCs to confirm the DNA damage-inducing potential of EA. As evident from the flow cytometry data in Figure 2H,I, EA treatment significantly induces γH2AX in CSLCs in a dose-dependent manner.

3.6. EA Treatment Induces Cell Death in Lung and Ovarian CSLCs. Initially, we investigated the effects of different doses of EA on lung and ovarian cancer cell lines. The colony formation assay results showed that the cell growth of SKOV3 and A549 cells was inhibited in a dose-dependent manner by EA treatment. Several natural compounds are known to inhibit cancer progression and metastasis, and EA is one of them.[25] Given that CSCs are responsible for cancer progression and metastasis, we sought to determine the therapeutic efficacy of EA against CSLCs. As shown by live−dead staining results using flow cytometry in Figure 3A,B, EA treatment induces significant cell death in A549-CD133$^+$ and SKOV3- spheroids in a dose-dependent manner. Furthermore, cell viability was assessed using a fluorescence microscope in A549-CD133$^+$ and SKOV3- spheroids following treatment with EA (0−50 μM) for 48 h, using PI (a red dye that stains the dead cells) and CFDA (a green fluorescent dye that stains the live cells). As anticipated, EA treatment (25 and 50 μM) resulted in higher proportion of cell killing, along with alternations in the size and morphology of spheroids Figure 3C,D.

3.7. EA Treatment Induces Apoptosis in CSLCs. Apoptosis, also known as programmed cell death, plays a crucial role in regulating cell development and normal cellular processes. This typical biological function becomes dysregulated in cancer, resulting in uncontrolled cell proliferation.[26] As mentioned earlier, anticancer chemotherapeutic agents induce cell death in proliferating tumor cells *via* activating apoptotic pathway but fail to inhibit tumor progression due to their inability to kill CSCs since they can escape apoptosis, resulting in tumor development.[27] Both apoptosis and necrosis are potential methods of cell death. From the live−dead test, we learned that EA treatment results in cell death. Nevertheless, we performed an Annexin V/PI assay to identify the molecular mechanism driving cell death (Figure 3E). We observed that EA treatment significantly increases the percentage of early and late apoptotic cells in a dose-dependent manner, further validating the apoptosis-inducing potential of EA in lung CSLCs. To understand the possible mechanism behind the pro-apoptotic activity of EA in CSLCs, changes in apoptotic protein expression were detected by western blot. The protein expression analysis confirmed the activation of p53 after EA treatment. EA (25 and 50 μM) significantly upregulated p53 expression in a concentration-dependent manner in both lung and ovarian CSLCs. Moreover, EA treatment significantly upregulated other pro-apoptotic proteins, such as cleaved caspase-3 (Figure 4A,B). Taken together, all of our data suggest that EA treatment limits the CSC population by inducing apoptosis.

3.8. Combinatorial Treatment of EA and Cisplatin Limits Cisplatin-Induced CSLCs Enrichment and Enhances the Efficacy of Cisplatin. As EA successfully reduced the levels of CD133$^+$ and CD44$^+$CD117$^+$ cells and enhanced cell death in CSLCs, our interest was raised in understanding the combinatorial effect exerted by EA and cisplatin on CSLCs. It has been shown that exposure to chemotherapeutic drugs such as cisplatin, oxaliplatin, and paclitaxel, enhances the proportion of cells with CSC properties, most likely due to the killing of drug-sensitive tumor cells and the survival of CSCs that exhibit drug-resistant properties.[28] To determine whether EA treatment blocks cisplatin-induced enrichment of CSCs, SKOV3,

https://doi.org/10.1021/acsomega.3c08819
ACS Omega 2024, 9, 48988−49000

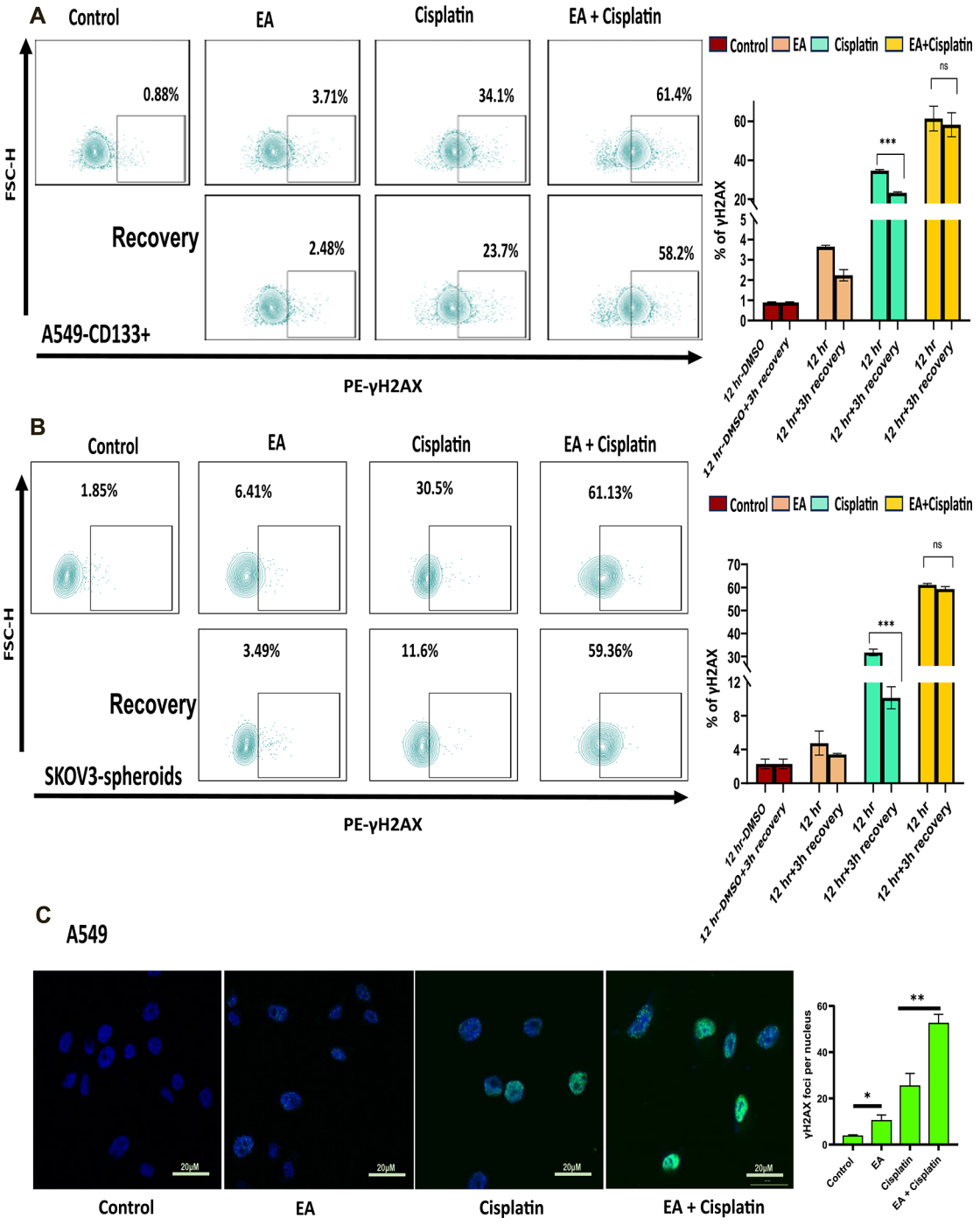

Figure 5. Combinatorial treatment of EA and cisplatin impairs DNA damage repair in lung and ovarian CSLCs. The DNA repair kinetics study depicts the percent DNA damage accumulation following DMSO, EA, cisplatin, and EA + cisplatin treatment for 12 h followed by 3 h damage recovery in (A) A549-CD133$^+$ and (B) SKOV3 spheroid cells. (C) The immunofluorescence staining shows the increasing accumulation of DNA damage in DMSO, EA, cisplatin, and EA + cisplatin-treated cells. The corresponding graph represents the mean fluorescence intensity of accumulated γH2AX. N=3, Bar, SD; *P < 0.05, **P < 0.01, and ***P < 0.001.

and A549, cells were treated with EA, cisplatin, or a combination of both (EA pretreatment + +cisplatin). The percentage of CD133$^+$ and CD44$^+$CD117$^+$ cells was determined by flow cytometry. As shown in Figure 4D,E, the combinatorial treatment limited the cisplatin-induced CSC enrichment significantly. Additionally, CSLCs were treated with DMSO, EA, cisplatin, and a combination of EA and cisplatin to examine the impact of combination treatment on these CSLCs. As shown in Figure 4F,G, more cell death was observed in the combination treatment group compared to EA and cisplatin alone groups, confirming that pretreatment of EA enhances the efficacy of cisplatin against CSLCs.

3.9. Combinatorial Treatment of EA and Cisplatin Enhances DNA Damage Accumulation and Impairs DNA Repair in CSLCs. Given that cisplatin induces cell death *via* causing DNA damage, we hypothesized that EA may enhance cisplatin-induced γH2AX formation. To test this hypothesis, the combinatorial effect of cisplatin and EA was

https://doi.org/10.1021/acsomega.3c08819
ACS Omega 2024, 9, 48988−49000

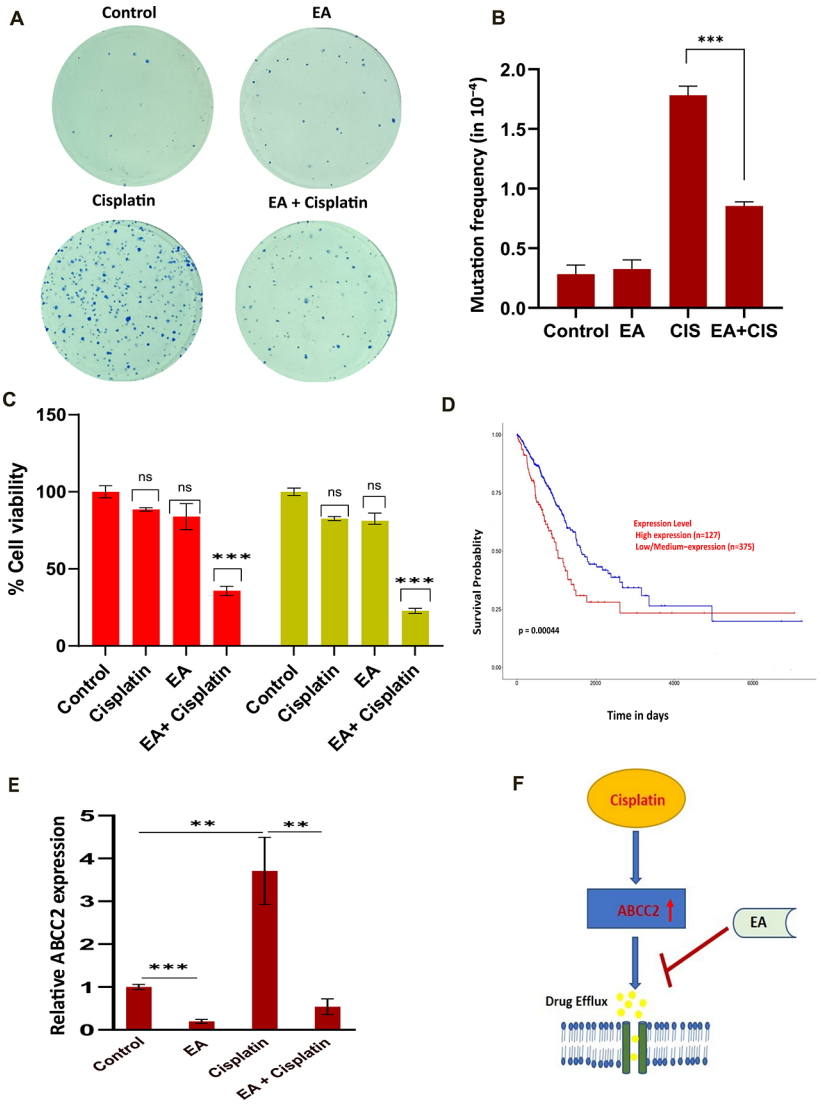

Figure 6. EA treatment reduces cisplatin-induced HPRT gene mutation frequency and overcomes cisplatin resistance probably by improving drug retention (A). HPRT assay showing the mutant colonies. (B) Graph indicating the HPRT mutation frequency observed after treatment with DMSO, EA, cisplatin, and EA + cisplatin. (C) Cell viability assay showing that EA treatment sensitizes the cisplatin-resistant C13 ovarian cancer cell line to cisplatin treatment. (D) Kaplan−Meier plot indicating an inverse correlation between ABCC2 expression and patient survival. P = 0.00044. (E) Real-time PCR expression analysis of ABCC2 in DMSO, cisplatin, EA, and EA + cisplatin-treated cells. (F) Schematic diagram showing that EA treatment could improve drug retention possibly *via* inhibiting ABCC2 expression in CSLCs. In all graphs, the results are represented as mean ± SD of the triplicate experiment. Bar, SD; $^{**}P < 0.01$, and SD; $^{***}P < 0.001$.

studied. Pretreatment of EA significantly increased the cisplatin-induced γH2AX foci formation in CSLCs compared to the cisplatin alone group, Figure 5A,B.

To demonstrate the effect of EA on the DNA repair ability of CSCs, a DNA repair kinetic study was performed. The level of γH2AX was detected by flow cytometry after allowing the cells to recover for 3 h following 12 h cisplatin treatment. As shown in Figure 5A,B, a significant reduction in levels of γH2AX accumulation was noticed in the 3 h recovery group following cisplatin alone treatment. However, an insignificant difference was noticed in the combination treatment group, *i.e.*, between cisplatin (12 h) + EA treatment *vs* 3 h recovery, indicating that EA treatment delayed the DNA repair and negatively impacted the progress of DNA break repair.

An immunofluorescence study also showed a similar result with a greater number of γH2AX accumulations in combination treatment compared to cisplatin alone, further confirming the therapeutic efficacy of EA against CSLCs (Figure 5C). Taken together, our result showed that pretreatment of EA impairs the repair process of cisplatin-induced DNA damage.

3.10. EA Treatment Reduces Cisplatin-Induced HPRT Gene Mutation Frequency. The accumulation of mutations is a prerequisite for the development of acquired drug resistance. Based on this scientific premise, we hypothesize that EA treatment might reduce chemotherapeutic drug-induced mutagenesis. To confirm this hypothesis, an HPRT assay was conducted. We investigated the ability of EA to decrease the cisplatin-induced HPRT gene mutation frequency in the A549 cell line. As shown in Figure 6A,B, an enhanced level of HPRT mutation was noticed in the cisplatin alone group compared to DMSO-treated cells. However, neither DMSO nor EA enhanced the HPRT mutation frequency, indicating that these compounds are nonmutagenic. Moreover,

https://doi.org/10.1021/acsomega.3c08819
ACS Omega 2024, 9, 48988−49000

EA pretreatment was able to reduce the cisplatin-induced HPRT gene mutation frequency significantly, indicating that EA inhibits the accumulation of mutation by depleting the mutant cells, and consequently could block chemoresistance. Similarly, we observed that pretreatment of EA sensitizes the cisplatin-resistant C13 ovarian cancer cell line to cisplatin treatment (Figure 6C). In summary, our data showed that EA treatment reduces cisplatin-induced mutagenesis, thus could block the development of chemoresistance.

3.11. EA Treatment Overcomes Cisplatin Resistance Possibly by Improving Drug Retention. Previous reports have suggested the involvement of efflux transporters such as ABC transporters in drug efflux , leading to chemoresistance.[29] Among the ABC transporters, the higher expression of ABCC2 is associated with cisplatin resistance in ovarian cancer.[30] The TCGA survival curve analysis using UALCAN (https://ualcan.path.uab.edu/analysis.html) revealed that a higher expression of ABCC2 is associated with poor survival in lung cancer patients[31] (Figure 6D). To investigate the impact of EA, cisplatin and their combination on ABCC2 expression in lung cancer, we performed qPCR analysis. Our analysis showed a ∼3.71-fold upregulation in ABCC2 expression following cisplatin alone treatment, whereas combinatorial treatment of EA + cisplatin downregulated the ABCC2 by ∼2-fold (Figure 6E) when compared to control group. Similarly, EA treatment alone reduced the ABCC2 levels by 5-fold. These results corroborate our hypothesis that EA indeed can reduce the development of chemoresistance, possibly *via* inhibiting ABCC2 transporter expression.

4. DISCUSSION

Several reports have confirmed the existence of CSCs as a subpopulation within tumor mass in different types of malignancies.[32] The ability of CSCs to become resistant to conventional anticancer drugs has led to a search for alternative therapeutics for cancer treatment. Several studies have outlined the value of *M. indica* in the management of various diseases. The Ayurvedic system of medicine has long been used *M. indica* to treat several illnesses[33−40] and is known to contain EA, a secondary metabolite also derived from different edible plant products that is effective in cancer treatment. Although the anticancer effects of EA have been extensively studied in various types of malignancies, there are only a few reports in ovarian cancer especially against CSCs. EA is known to block drug resistance *via* inhibiting P-glycoprotein drug efflux activity.[41] Thus, EA is a credible option for usage against the CSCs, either alone or in conjunction with other anticancer medications. Previous studies have shown the inhibitory role of EA in proliferation, arresting cell cycle, and enhancing apoptosis in human osteosarcoma and breast cancer.[42,43] EA treatment causes a reduction in breast cancer metastasis through the β-catenin stabilization in CSCs.[25] In this study, we analyzed the effect caused by purified EA on the stemness property of CSCs and its ability to block chemoresistance.

Our data revealed that EA treatment causes the depletion of CSLCs exhibiting stemness and drug-resistant phenotypes. The reduction of stem cell properties of CSCs results in lower self-renewal ability, hence reducing the chances of tumor relapse. Our data suggest that EA reduces the cisplatin-induced enrichment of CSCs in both lung and ovarian cancers, indicating the CSCs sensitizing ability of EA. Furthermore, we confirmed the cytotoxic effect of EA on CSCs through live−dead assay using flow cytometry, where we observed that the CSCs exhibit significant sensitivity toward EA treatment at higher doses. A similar cytotoxic effect of EA was also revealed by the cell viability assay. Additionally, our results revealed that EA treatment induces enhanced apoptosis at higher concentrations, indicating the pro-apoptotic role of EA in both lung and ovarian CSLCs. ROS ($O^{2\bullet-}$, $OH^{\bullet}$, H_2O_2, *etc.*) at low to modest levels regulate normal physiological functions. When it accumulates at a higher level, it causes oxidative stress, and excess ROS can damage nucleic acids, proteins, lipids, membranes, *etc.*[44] EA treatment induces the increased accumulation of ROS in the CSLCs, thus triggering the activation of the apoptotic pathway in CSLCs *via* enhancing DNA damage. In the same line, a previous report has shown the role of EA in blocking the DNA damage repair by inhibiting the DNA polymerase (eta) η and (iota) ι,[45] which may lead to accumulation of the DNA damage and activation of apoptotic pathways. We further checked the status of mitochondrial dynamics regulators after EA treatment in ovarian CSLCs. Our findings suggest that EA alters the mitochondrial dynamics regulator's protein expression such as Drp1 and Mfn2. It is known that mitochondrial dynamics are closely linked to mitochondrial morphology, regulating mitochondrial functions. It is a given that the mitochondrial fission and fusion processes impact the ROS generation.[23] ROS-mediated DNA damage can activate the p53 and ERK pathway, which might induce apoptosis.[46,47] To this end, we demonstrated higher expressions of p-ERK and p53 in CSLCs following EA treatment. Our study has shown that EA treatment results in an increased accumulation of cleaved caspase-3, which signifies the induction of apoptosis. It has already been reported that EA can ameliorate the nephrotoxicity caused by cisplatin administration in cancer patients[48], thereby increases the efficacy of cisplatin. However, in this study, we have shown that EA also blocks the cisplatin-induced enrichment of CSCs as indicated by reduced $CD133^+$ and $CD44^+CD117^+$ percentage in FACS analysis upon combinatorial treatment of cisplatin with EA compared to cisplatin treatment only. Further, the combinatorial treatment of EA with cisplatin was also able to reduce the DNA repair ability of the CSCs. In addition, EA treatment significantly blocked the expression levels of ABCC2, a drug efflux transporter. The ability of EA to reduce ABCC2 expression in CSLCs provides an opportunity to increase cisplatin retention within the CSCs and therefore could enhance the drug efficacy.

5. CONCLUSIONS

In conclusion, EA displayed the potential to selectively eradicate CSCs. EA alters the mitochondrial dynamics, causing enhanced ROS production and an increase in DNA damage, which leads to the activation of apoptotic pathways in CSLCs. Moreover, pretreatment of EA sensitizes CSLCs to cisplatin treatment. Thus, EA could be used as a promising therapeutic agent either alone or as an adjuvant therapy for cancer treatment. Combining EA with other platinum-based drugs, *e.g.*, cisplatin, may not only reduce the toxicity induced by conventional chemotherapeutic drugs, but also could improve the drug retention, thereby enhancing the efficacy of chemotherapeutic drugs.

https://doi.org/10.1021/acsomega.3c08819
ACS Omega 2024, 9, 48988−49000

■ ASSOCIATED CONTENT

Supporting Information

The Supporting Information is available free of charge at https://pubs.acs.org/doi/10.1021/acsomega.3c08819.

ESI-MS, NMR, and HPLC data of ellagic acid, isolation and characterization of CSCs, and cytotoxicity of EA and raw immunoblots (PDF)

■ AUTHOR INFORMATION

Corresponding Author

Amit Kumar Srivastava − *Cancer Biology & Inflammatory Disorder Division, CSIR-Indian Institute of Chemical Biology, Kolkata, West Bengal 700032, India; Academy of Scientific and Innovative Research (AcSIR), Ghaziabad 201002, India;* orcid.org/0000-0002-4941-0591; Email: amit@iicb.res.in

Authors

Tanima Mandal − *Cancer Biology & Inflammatory Disorder Division, CSIR-Indian Institute of Chemical Biology, Kolkata, West Bengal 700032, India; Academy of Scientific and Innovative Research (AcSIR), Ghaziabad 201002, India*

Devendra Shukla − *Cancer Biology & Inflammatory Disorder Division, CSIR-Indian Institute of Chemical Biology, Kolkata, West Bengal 700032, India; Academy of Scientific and Innovative Research (AcSIR), Ghaziabad 201002, India*

Subhamoy Pattanayak − *Organic and Medicinal Chemistry Division, CSIR-Indian Institute of Chemical Biology, Kolkata, West Bengal 700032, India*

Raju Barman − *Organic and Medicinal Chemistry Division, CSIR-Indian Institute of Chemical Biology, Kolkata, West Bengal 700032, India*

Rahail Ashraf − *Division of Biology, Indian Institute of Science Education & Research Tirupati, Tirupati, Andhra Pradesh 517507, India*

Amit Kumar Dixit − *CCRAS-Central Ayurveda Research Institute, Kolkata, West Bengal 700091, India*

Sanjay Kumar − *Division of Biology, Indian Institute of Science Education & Research Tirupati, Tirupati, Andhra Pradesh 517507, India*

Deepak Kumar − *Organic and Medicinal Chemistry Division, CSIR-Indian Institute of Chemical Biology, Kolkata, West Bengal 700032, India; Academy of Scientific and Innovative Research (AcSIR), Ghaziabad 201002, India*

Complete contact information is available at: https://pubs.acs.org/10.1021/acsomega.3c08819

Author Contributions

T.M. and D.S. contributed equally. **Tanima Mandal** and **Devendra Shukla** performed the conceptualization, methodology, investigation, formal analysis, and writing—original draft; **Subhamoy Pattanayak**, **Raju Barman**, and **Rahail Ashraf** carried out the investigation; **Amit Kumar Dixit** executed the reviewing and editing; **Deepak Kumar** and **Sanjay Kumar** performed the conceptualization, methodology, and resource procurement; **Amit Kumar Srivastava** participated in the conceptualization, resource procurement, investigation, formal analysis, validation, and writing—reviewing and editing.

Funding

The study was supported by CCRAS, Ministry of Ayush (Office Order no. 1306/2022-23 dated 23/02/2023) and internal funding (P07) of CSIR-IICB, Kolkata

Notes

The authors declare no competing financial interest.

■ ACKNOWLEDGMENTS

T.M. and D.S. are recipients of a Senior Research Fellowship from CSIR. The authors express gratitude to Prof. Qi-En Wang and Prof. Ramesh Ganju from The Ohio State University for generously providing the cell lines. R.B. received fellowship from MLP-138 (CSIR).

■ ABBREVIATIONS

ABCC2, ATP binding cassette subfamily C member 2; CSCs, cancer stem cells; Drp1, dynamin-related protein 1; EA, ellagic acid; γH2AX, gamma H2A histone family member X; Mfn2, mitofusin 2

■ REFERENCES

(1) Ferlay, J.; Colombet, M.; Soerjomataram, I.; Parkin, D. M.; Piñeros, M.; Znaor, A.; Bray, F. Cancer statistics for the year 2020: An overview. *Int. J. Cancer* **2021**, *149* (4), 778−789.

(2) Ramos, A.; Sadeghi, S.; Tabatabaeian, H. Battling chemoresistance in cancer: Root causes and strategies to uproot them. *Int. J. Mol. Sci.* **2021**, *22*, 9451.

(3) Yang, Z. J.; Wechsler-Reya, R. J. Hit 'Em Where They Live: Targeting the Cancer Stem Cell Niche. *Cancer Cell* **2007**, *11* (1), 3−5.

(4) Molyneux, R. J.; Lee, S. T.; Gardner, D. R.; Panter, K. E.; James, L. F. Phytochemicals: The good, the bad and the ugly? *Phytochemistry* **2007**, *68* (22−24), 2973−2985.

(5) Choudhari, A. S.; Mandave, P. C.; Deshpande, M.; Ranjekar, P.; Prakash, O. Phytochemicals in Cancer Treatment: From Preclinical Studies to Clinical Practice. *Front. Pharmacol* **2020**, *10*, 1614.

(6) Milivojević, J.; Maksimović, V.; Nikolić, M.; Bogdanović, J.; Maletić, R.; Milatović, D. Chemical and Antioxidant Properties of Cultivated and Wild Fragaria and Rubus Berries. *J. Food Qual.* **2011**, *34* (1), 1−9.

(7) Ribeiro, B.; Valentão, P.; Baptista, P.; Seabra, R. M.; Andrade, P. B. Phenolic compounds, organic acids profiles and antioxidative properties of beefsteak fungus (Fistulina hepatica). *Food Chem. Toxicol.* **2007**, *45* (10), 1805−1813.

(8) Yadollahi, E.; Shareghi, B.; Farhadian, S.; Hashemi Shahraki, F. Evaluation of the binding behavior of ellagic acid with Trypsin: Spectroscopic and computational studies. *J. Mol. Liq.* **2023**, *391*, 123338.

(9) Espín, J. C.; Larrosa, M.; García-Conesa, M. T.; Tomás-Barberán, F. Biological Significance of Urolithins, the Gut Microbial Ellagic Acid-Derived Metabolites: The Evidence So Far. *Evid. Base Compl. Alternative Med.* **2013**, *2013*, 270418.

(10) Giménez-Bastida, J. A.; Larrosa, M.; González-Sarrías, A.; Tomás-Barberán, F.; Espín, J. C.; García-Conesa, M. T. Intestinal Ellagitannin Metabolites Ameliorate Cytokine-Induced Inflammation and Associated Molecular Markers in Human Colon Fibroblasts. *J. Agric. Food Chem.* **2012**, *60* (36), 8866−8876.

(11) González-Sarrías, A.; Tomé-Carneiro, J.; Bellesia, A.; Tomás-Barberán, F. A.; Espín, J. C. The ellagic acid-derived gut microbiota metabolite, urolithin A, potentiates the anticancer effects of 5-fluorouracil chemotherapy on human colon cancer cells. *Food Funct.* **2015**, *6* (5), 1460−1469.

(12) Lopez, J. S.; Banerji, U. Combine and conquer: challenges for targeted therapy combinations in early phase trials. *Nat. Rev. Clin. Oncol.* **2017**, *14* (1), 57−66.

https://doi.org/10.1021/acsomega.3c08819
ACS Omega 2024, 9, 48988−49000

(13) Dasari, S.; Bernard Tchounwou, P. Cisplatin in cancer therapy: Molecular mechanisms of action. *Eur. J. Pharmacol.* **2014**, *740*, 364−378.
(14) Pecorelli, S.; Favalli, G.; Zigliani, L.; Odicino, F. Cancer in women. *Int. J. Gynecol. Obstet.* **2003**, *82* (3), 369−379.
(15) Murphy, M.; Stordal, B. Erlotinib or gefitinib for the treatment of relapsed platinum pretreated non-small cell lung cancer and ovarian cancer: A systematic review. *Drug Resist. Updates* **2011**, *14* (3), 177−190.
(16) Soong, Y. Y.; Barlow, P. J. Quantification of gallic acid and ellagic acid from longan (Dimocarpus longan Lour.) seed and mango (Mangifera indica L.) kernel and their effects on antioxidant activity. *Food Chem.* **2006**, *97* (3), 524−530.
(17) Zhu, W.; Yamasaki, H.; Mironov, N. Frequency of HPRT gene mutations induced by N-methyl-N′-nitro-N-nitrosoguanidine corresponds to replication error phenotypes of cell lines. *Mutation Research* **1998**, *398* (1−2), 93−99.
(18) Li, X. C.; Elsohly, H. N.; Hufford, C. D.; Clark, A. M. NMR assignments of ellagic acid derivatives. *Magn. Reson. Chem.* **1999**, *37*, 856−859.
(19) Luo, X.; Dong, Z.; Chen, Y.; Yang, L.; Lai, D. Enrichment of ovarian cancer stem-like cells is associated with epithelial to mesenchymal transition through an miRNA-activated AKT pathway. *Cell Prolif.* **2013**, *46* (4), 436−446.
(20) Sarvi, S.; Mackinnon, A. C.; Avlonitis, N.; Bradley, M.; Rintoul, R. C.; Rassl, D. M.; Wang, W.; Forbes, S. J.; Gregory, C. D.; Sethi, T. CD133+ Cancer Stem-like Cells in Small Cell Lung Cancer Are Highly Tumorigenic and Chemoresistant but Sensitive to a Novel Neuropeptide Antagonist. *Cancer Res.* **2014**, *74* (5), 1554−1565.
(21) Srivastava, A. K.; Rizvi, A.; Cui, T.; Han, C.; Banerjee, A.; Naseem, I.; et al. Depleting ovarian cancer stem cells with calcitriol. *Oncotarget* **2018**, *9*, 14481−14491.
(22) Loh, Y. H.; Wu, Q.; Chew, J. L.; Vega, V. B.; Zhang, W.; Chen, X.; Bourque, G.; George, J.; Leong, B.; Liu, J.; et al. The Oct4 and Nanog transcription network regulates pluripotency in mouse embryonic stem cells. *Nat. Genet.* **2006**, *38* (4), 431−440.
(23) Ashraf, R.; Kumar, S. Mfn2-mediated mitochondrial fusion promotes autophagy and suppresses ovarian cancer progression by reducing ROS through AMPK/mTOR/ERK signaling. *Cell. Mol. Life Sci.* **2022**, *79* (11), 573.
(24) Mukherjee, B.; Kessinger, C.; Kobayashi, J.; Chen, B. P. C.; Chen, D. J.; Chatterjee, A.; Burma, S. DNA-PK phosphorylates histone H2AX during apoptotic DNA fragmentation in mammalian cells. *DNA Repair* **2006**, *5* (5), 575−590.
(25) Wang, N.; Wang, Q.; Tang, H.; Zhang, F.; Zheng, Y.; Wang, S.; Zhang, J.; Wang, Z.; Xie, X. Direct inhibition of ACTN4 by ellagic acid limits breast cancer metastasis via regulation of β-catenin stabilization in cancer stem cells. *J. Exp. Clin. Cancer Res.* **2017**, *36* (1), 172.
(26) Mohammad, R. M.; Muqbil, I.; Lowe, L.; Yedjou, C.; Hsu, H. Y.; Lin, L. T.; Siegelin, M. D.; Fimognari, C.; Kumar, N. B.; Dou, Q. P.; et al. Broad targeting of resistance to apoptosis in cancer. *Semin. Cancer Biol.* **2015**, *35*, S78−S103.
(27) Safa, A. R. Drug and apoptosis resistance in cancer stem cells: a puzzle with many pieces. *Cancer Drug Resist.* **2022**, *5*, 850−872.
(28) Abubaker, K.; Latifi, A.; Luwor, R.; Nazaretian, S.; Zhu, H.; Quinn, M. A.; Thompson, E. W.; Findlay, J. K.; Ahmed, N. Short-term single treatment of chemotherapy results in the enrichment of ovarian cancer stem cell-like cells leading to an increased tumor burden. *Mol. Cancer* **2013**, *12* (1), 24.
(29) Dean, M. ABC Transporters, Drug Resistance, and Cancer Stem Cells. *J. Mammary Gland Biol. Neoplasia* **2009**, *14* (1), 3−9.
(30) Surowiak, P.; Materna, V.; Kaplenko, I.; Spaczynski, M.; Dolinska-Krajewska, B.; Gebarowska, E.; Dietel, M.; Zabel, M.; Lage, H. ABCC2 (MRP2, cMOAT) Can Be Localized in the Nuclear Membrane of Ovarian Carcinomas and Correlates with Resistance to Cisplatin and Clinical Outcome. *Clin. Cancer Res.* **2006**, *12* (23), 7149−7158.
(31) Chandrashekar, D. S.; Karthikeyan, S. K.; Korla, P. K.; Patel, H.; Shovon, A. R.; Athar, M.; Netto, G. J.; Qin, Z. S.; Kumar, S.; Manne, U.; et al. UALCAN: An update to the integrated cancer data analysis platform. *Neoplasia* **2022**, *25*, 18−27.
(32) Jordan, C. T.; Guzman, M. L.; Noble, M. Cancer Stem Cells. *N. Engl. J. Med.* **2006**, *355* (12), 1253−1261.
(33) Ferreira Gomes, C. C.; Siqueira Oliveira, L.; Rodrigues, D. C.; Ribeiro, P. R. V.; Canuto, K. M.; Duarte, A. S. G.; Eça, K. S.; Figueiredo, R. W. Evidence for antioxidant and anti-inflammatory potential of mango (Mangifera indica L.) in naproxen-induced gastric lesions in rat. *J. Food Biochem.* **2022**, *46* (3), No. e13880.
(34) Kulkarni, V. M.; Rathod, V. K. Exploring the potential of Mangifera indica leaves extract versus mangiferin for therapeutic application. *Agric. Nat. Resour.* **2018**, *52* (2), 155−161.
(35) Makare, N.; Bodhankar, S.; Rangari, V. Immunomodulatory activity of alcoholic extract of Mangifera indica L. in mice. *J. Ethnopharmacol.* **2001**, *78* (2−3), 133−137.
(36) Mirza, B.; Croley, C. R.; Ahmad, M.; Pumarol, J.; Das, N.; Sethi, G.; Bishayee, A. Mango (Mangifera indica L.): a magnificent plant with cancer preventive and anticancer therapeutic potential. *Crit. Rev. Food Sci. Nutr.* **2021**, *61* (13), 2125−2151.
(37) Mohan, C. G.; Deepak, M.; Viswanatha, G. L.; Savinay, G.; Hanumantharaju, V.; Rajendra, C. E.; Halemani, P. D. Anti-oxidant and anti-inflammatory activity of leaf extracts and fractions of Mangifera indica. *Asian Pac. J. Trop. Med.* **2013**, *6* (4), 311−314.
(38) Morvin Yabesh, J. E.; Prabhu, S.; Vijayakumar, S. An ethnobotanical study of medicinal plants used by traditional healers in silent valley of Kerala, India. *J. Ethnopharmacol.* **2014**, *154* (3), 774−789.
(39) Samoisy, A. K.; Mahomoodally, F. Ethnopharmacological appraisal of culturally important medicinal plants and polyherbal formulas used against communicable diseases in Rodrigues Island. *J. Ethnopharmacol.* **2016**, *194*, 803−818.
(40) Yakubu, M. T.; Salimon, S. S. Antidiarrhoeal activity of aqueous extract of Mangifera indica L. leaves in female albino rats. *J. Ethnopharmacol.* **2015**, *163*, 135−141.
(41) Eskra, J. N.; Schlicht, M. J.; Bosland, M. C. Effects of Black Raspberries and Their Ellagic Acid and Anthocyanin Constituents on Taxane Chemotherapy of Castration-Resistant Prostate Cancer Cells. *Sci. Rep.* **2019**, *9* (1), 4367.
(42) Chen, H. S.; Bai, M. H.; Zhang, T.; Li, G. D.; Liu, M. Ellagic acid induces cell cycle arrest and apoptosis through TGF-β/Smad3 signaling pathway in human breast cancer MCF-7 cells. *Int. J. Oncol.* **2015**, *46* (4), 1730−1738.
(43) Zhang, H. M.; Zhao, L.; Li, H.; Xu, H.; Chen, W. W.; Tao, L. Research progress on the anticarcinogenic actions and mechanisms of ellagic acid. *Cancer Biol. Med.* **2014**, *11*, 92−100.
(44) Redza-Dutordoir, M.; Averill-Bates, D. A. Activation of apoptosis signalling pathways by reactive oxygen species. *Biochim. Biophys. Acta, Mol. Cell Res.* **2016**, *1863*, 2977−2992.
(45) Dorjsuren, D.; Wilson, D. M.; Beard, W. A.; McDonald, J. P.; Austin, C. P.; Woodgate, R.; Wilson, S. H.; Simeonov, A. A real-time fluorescence method for enzymatic characterization of specialized human DNA polymerases. *Nucleic Acids Res.* **2009**, *37* (19), No. e128.
(46) Cagnol, S.; Chambard, J. C. ERK and cell death: Mechanisms of ERK-induced cell death - apoptosis, autophagy and senescence. *FEBS J.* **2010**, *277* (1), 2−21.
(47) Tang, D.; Wu, D.; Hirao, A.; Lahti, J. M.; Liu, L.; Mazza, B.; Kidd, V. J.; Mak, T. W.; Ingram, A. J. ERK Activation Mediates Cell Cycle Arrest and Apoptosis after DNA Damage Independently of p53*. *J. Biol. Chem.* **2002**, *277* (15), 12710−12717.
(48) Goyal, Y.; Koul, A.; Ranawat, P. Ellagic acid ameliorates cisplatin toxicity in chemically induced colon carcinogenesis. *Mol. Cell. Biochem.* **2019**, *453* (1−2), 205−215.

https://doi.org/10.1021/acsomega.3c08819
ACS Omega 2024, 9, 48988−49000